Proc. Natl. Acad. Sci. USA
Vol. 93, pp. 5495–5500, May 1996
Physiology

Cellular and subcellular localization of the vasopressin-regulated urea transporter in rat kidney

SØREN NIELSEN*, JAMES TERRIS†‡, CRAIG P. SMITH†, MATTHIAS A. HEDIGER§, CAROLYN A. ECELBARGER†, AND MARK A. KNEPPER†¶

*Department of Cell Biology, University of Aarhus, DK-8000 Aarhus C, Denmark; †Laboratory of Kidney and Electrolyte Metabolism, National Heart, Lung, and Blood Institute, National Institutes of Health, Bethesda, MD 20892; §Renal Division, Brigham and Women's Hospital and Harvard Medical School, Boston, MA 02115; and ‡Department of Physiology, Uniformed Services University of Health Sciences, Bethesda, MD 20814

Communicated by Robert W. Berliner, Yale University School of Medicine, New Haven, CT, January 29, 1996 (received for review December 1, 1995)

ABSTRACT **The renal urea transporter (RUT) is responsible for urea accumulation in the renal medulla, and consequently plays a central role in the urinary concentrating mechanism. To study its cellular and subcellular localization, we prepared affinity-purified, peptide-derived polyclonal antibodies against rat RUT based on the cloned cDNA sequence. Immunoblots using membrane fractions from rat renal inner medulla revealed a solitary 97-kDa band. Immunocytochemistry demonstrated RUT labeling of the apical and subapical regions of inner medullary collecting duct (IMCD) cells, with no labeling of outer medullary or cortical collecting ducts. Immunoelectron microscopy directly demonstrated labeling of the apical plasma membrane and of subapical intracellular vesicles of IMCD cells, but no labeling of the basolateral plasma membrane. Immunoblots demonstrated RUT labeling in both plasma membrane and intracellular vesicle-enriched membrane fractions from inner medulla, a subcellular distribution similar to that of the vasopressin-regulated water channel, aquaporin-2. In the outer medulla, RUT labeling was seen in terminal portions of short- loop descending thin limbs. Aside from IMCD and descending thin limbs, no other structures were labeled in the kidney. These results suggest that: (*i*) the RUT provides the apical pathway for rapid, vasopressin-regulated urea transport in the IMCD, (*ii*) collecting duct urea transport may be increased by vasopressin by stimulation of trafficking of RUT-containing vesicles to the apical plasma membrane, and (*iii*) the rat urea transporter may provide a pathway for urea entry into the descending limbs of short-loop nephrons.**

Rapid, passive urea absorption from the inner medullary collecting duct (IMCD) is responsible for generation of high urea concentrations in the inner medullary interstitium (1) and consequently plays a central role in the urinary concentrating mechanism (2). The rate of absorption is accelerated by vasopressin (3, 4) via increases in intracellular cyclic AMP (5). Physiological studies in isolated perfused tubules have demonstrated that this urea transport pathway is inhibitable by phloretin and structural analogs of urea (6), and is saturable (7), providing strong evidence for the presence of a facilitated urea transporter in IMCD cells (8). Although urea transport across both apical and basolateral plasma membranes of IMCD cells appears to be mediated by phloretin-sensitive urea transporters (6, 9), urea transport across the apical plasma membrane is rate-limiting for overall transepithelial urea transport and is regulated by vasopressin (9). The mechanism by which vasopressin increases urea transport across the apical plasma membrane of the IMCD has not been investigated. In general, there are two possible mechanisms. (*i*) As has been demonstrated for the vasopressin-regulated water channel (10–13), the urea permeability of the apical plasma membrane may be increased as a result of vasopressin-stimulated insertion of urea-transporter-containing vesicles into the apical plasma membrane. (*ii*) Urea transporters may reside constitutively in the apical membrane and may be activated by posttranslational modification—e.g., phosphorylation by protein kinase A.

Recently, a cDNA coding for a phloretin-sensitive renal urea transporter (RUT) was cloned by Hediger and associates in rabbit (14) and rat (15). Expression of RUT in *Xenopus* oocytes conferred the oocytes with phloretin-inhibitable urea transport and *in situ* hybridization revealed strong signals in IMCD, consistent with the tentative identification of RUT as the vasopressin-regulated urea transporter of the collecting ducts. In addition, *in situ* hybridization revealed the presence of RUT mRNA in unidentified structures in the inner stripe of outer medulla.

These studies were undertaken to determine the cellular and subcellular localization of RUT using peptide-directed polyclonal antibodies to the carboxyl-terminal tail of RUT. The chief objectives were: (*i*) to identify whether the localization of RUT is consistent with its proposed role as the vasopressin-regulated urea transporter of the apical plasma membrane of IMCD; (*ii*) to determine whether the subcellular distribution of RUT in IMCD cells is consistent with the view that transport via RUT may be regulated by shuttling of RUT-containing intracellular vesicles to and from the apical plasma membrane; and (*iii*) to identify the structures in the outer medulla that contain RUT.

MATERIALS AND METHODS

Preparation of Antibodies. Polyclonal antisera were raised in rabbits against an HPLC-purified synthetic peptide corresponding to the carboxyl-terminal 19 amino acids of rat RUT, based on the sequence reported by Smith *et al.* (15). The peptide was synthesized with the addition of a cysteine residue at the amino terminus to facilitate conjugation to a carrier protein, keyhole limpet hemocyanin, via a cysteine sulfhydryl linkage. Two rabbits were immunized with the peptide-keyhole limpet hemocyanin conjugate as described (16). Both rabbits (LL193 and LL194) developed ELISA titers of >1:32,000. The antisera were affinity purified using a column on which 2 mg of the synthetic peptide was immobilized via sulfhydryl linkage to activated agarose beads (SulfoLink Immunobilization Kit 2, Pierce). Although the two antisera gave similar labeling on

The publication costs of this article were defrayed in part by page charge payment. This article must therefore be hereby marked "*advertisement*" in accordance with 18 U.S.C. §1734 solely to indicate this fact.

Abbreviations: RUT, renal urea transporter; IMCD, inner medullary collecting duct; DTL, descending thin limb.

¶To whom reprint requests should be addressed at: National Heart, Lung, and Blood Institute/Laboratory of Kidney and Electrolyte Metabolism, Building 10, Room 6N307, 10 Center Drive MSC 1598, National Institutes of Health, Bethesda, MD 20892-1598. e-mail: knep@helix.nih.gov.

both immunoblots and immunocytochemistry, the studies reported here were carried out with antiserum LL194. Affinity-purified antibodies to aquaporin-2 and aquaporin-3 have been described (17, 18).

Membrane Fractionation. Cortex, outer medulla, and inner medulla were dissected from each kidney, minced finely, and homogenized in isolation solution (250 mM sucrose/10 mM triethanolamine, pH 7.6) containing protease inhibitors (1 μg/ml leupeptin and 0.1 mg/ml phenylmethylsulfonyl fluoride). Crude membrane fractions were obtained by centrifuging at 1000 × *g* for 10 min at 4°C, discarding the pellet and centrifuging the supernatant at 17,000 × *g* at 4°C for 20 min. The resulting pellet was resuspended in isolation solution and protein concentrations were determined using the Pierce BCA Protein Assay kit. These samples were solubilized in Laemmli sample buffer as previously described (16, 17).

For subcellular fractionation, sequential centrifugations of the homogenates were carried out at 1000 × *g* for 10 min, 4000 × *g* for 20 min, 17,000 × *g* for 20 min, and 200,000 × *g* for 60 min (11, 18). After total protein determination, the pellets from these centrifugations were solubilized in Laemmli sample buffer.

Electrophoresis and Immunoblotting of Membrane Proteins. Membrane samples were loaded at 1–10 μg per lane on SDS/12% PAGE minigels and electrophoresed using an XCell II mini-cell (NOVEX, San Diego). Proteins were transferred to nitrocellulose membranes by electroelution using a Bio-Rad Mini-Trans-Blot cell. The blots were blocked for 1 hr with 5% nonfat dry milk in PBS-T (80 mM/Na_2HPO_4/20 mM NaH_2PO_4/100 mM NaCl/0.1% Tween 20, pH 7.5), washed and incubated overnight at 4°C with anti-RUT (IgG concentration, 372–744 ng/ml) in PBS-T with 1% BSA. After washing, the blots were incubated for 1 hr with donkey anti-rabbit secondary antibody conjugated to horseradish peroxidase (160 ng/ml, Pierce no. 31458), and antibody binding was visualized using luminol-based enhanced chemiluminescence (LumiGLO; Kirkegaard & Perry Laboratories) before exposure to imaging film (Kodak 165-1579 scientific imaging film).

Immunocytochemistry. Immunocytochemistry was performed as described (11, 16, 17). Rat kidneys were perfusion fixed with 8% paraformaldehyde in 0.1 M sodium cacodylate buffer at pH 7.2. Tissue blocks prepared from the kidney inner medulla and inner stripe of the outer medulla were postfixed in the same fixative for 2 hr and then were infiltrated for 30 min with 2.3 M sucrose containing 2% paraformaldehyde. The blocks were mounted on holders and rapidly frozen in liquid nitrogen. Thin (0.85 μm) and ultrathin (80 nm) cryosections were preincubated with PBS containing 1% BSA and 0.05 M glycine, and incubated overnight at 5°C with anti-RUT antibody (LL194, 2–4 μg/ml of IgG in PBS). For standard immunocytochemistry in thin sections the labeling was visualized by use of a horseradish peroxidase-conjugated secondary antibody (P448, 1:100, Dako) as described (16). For immunoelectron microscopy, RUT labeling was visualized using goat anti-rabbit gold (10-nm gold particles, EM.GAR10, 1:50, BioCell Research Laboratories, Cardiff, U.K.) as described (11).

RESULTS

The specificity of the affinity-purified anti-RUT antibody was assessed by immunoblotting using a crude membrane fraction (17,000 × *g* pellet) from rat kidney inner medulla (Fig. 1*A*). The antibody recognized a solitary band with a mobility corresponding to a molecular mass of approximately 97 kDa. This molecular mass is consistent with the expected size of the collecting duct form of the RUT protein based on cDNA cloning (see *Discussion*). When immunoblots were probed with anti-RUT preadsorbed with the immunizing peptide (Fig. 1*A*) the band was absent. In addition, no bands were seen when the IgG fraction of the preimmune serum was used instead of the primary antibody or when the primary antibody was omitted (not shown). Fig. 1*B* shows the regional distribution of RUT in the rat kidney as determined by immunoblotting of crude membrane preparations (17,000 × *g* pellet) from cortex, outer medulla, and from the base and tip of the inner medulla. There was detectable RUT expression only in the inner medulla, with the greatest level of expression in the deepest part of the inner medulla (inner medullary tip). Localization in the inner medulla was confirmed using membranes from the whole inner medulla of a different rat (right-hand lane). Blots run with membranes treated with 6 M urea and/or boiling revealed the same 97 kDa band with no additional bands (not shown).

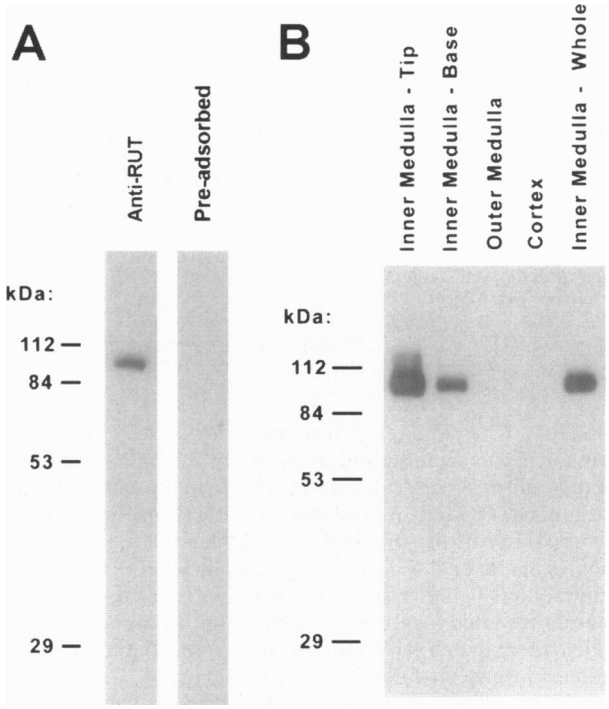

FIG. 1. Renal immunoblots using affinity-purified anti-RUT. (*A*) Blots were run with 5 μg of protein per lane of crude membrane fraction (17,000 × *g* pellet) from inner medulla and probed with affinity-purified anti-RUT antibody (LL194, 740 ng/ml of IgG) or with the same antibody preadsorbed with an excess of the immunizing peptide. (*B*) Individual lanes were loaded with crude membrane fraction (17,000 × *g* pellet) from various regions of rat kidney (10 μg of protein per lane). Immunoblots were probed with affinity-purified antibody (LL194, IgG concentration, 740 ng/ml). A 97-kDa band was seen only in the inner medulla (tip > base).

The cellular distribution was examined by immunocytochemistry using semithin cryosections (Fig. 2). In the outer half of the kidney inner medulla (Fig. 2*A*) collecting ducts exhibited abundant labeling in the apical region of IMCD principal cells. Incubation with nonimmune IgG (not shown) or affinity-purified antibody preadsorbed with an excess of immunizing peptide (Fig. 2 *H* and *I*) revealed an absence of labeling. Higher magnification revealed labeling associated with both apical plasma membranes and subapical domains of principal cells with no labeling of basolateral regions (Fig. 2*B*). Collecting duct cells from deeper portions of the inner medulla (Fig. 2*C*) also exhibited extensive labeling of plasma membranes and vesicles. In contrast to the substantial labeling in the collecting ducts throughout most of the inner medulla (Fig. 2 *A*–C), collecting duct principal cells in the outer 1 mm of the inner medulla exhibited considerably less labeling (not shown). This finding is consistent with the immunoblotting showing higher RUT-labeling in tip versus base of the inner medulla (Fig. 1*A*).

Thin limbs and vascular structures were unlabeled throughout the inner medulla (Fig. 2*A*–2*C*). Also, the surface epithelium separating the parenchyma of the medulla from the pelvic space exhibited no RUT labeling (Fig. 2*D*).

Earlier studies using *in situ* hybridization provided evidence for RUT mRNA in unidentified structures in the outer medulla (14, 15). Immunocytochemistry in the outer medulla of rats (Fig. 2 *D*–*G*), revealed distinct RUT labeling of descending thin limbs of short-loop nephrons. In contrast, there was no labeling of collecting duct principal or intercalated cells, long-loop descending thin limbs, vasa recta, or thick ascending limbs in the outer medulla (Fig. 2 *D*–*G*). The labeling of outer medullary thin limbs was especially evident in the region close to the inner–outer medullary junction (Fig. 2*D*). Observations at high magnification revealed predominant labeling of the terminal part of the short-loop descending thin limb, as evidenced by abrupt transitions of labeled thin limb segments into unlabeled thick ascending limbs (Fig. 2 *E* and *F*). Fur-

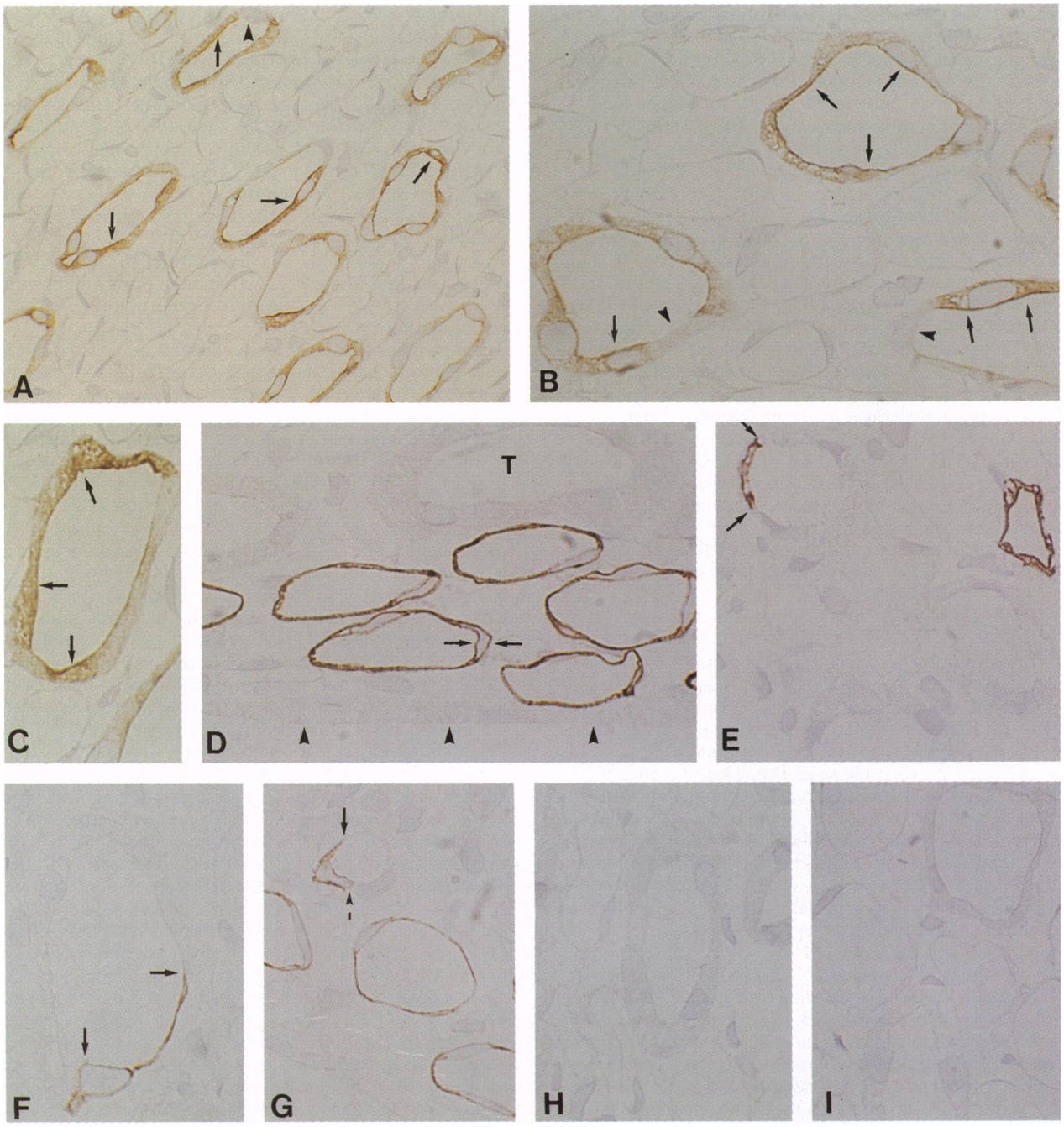

FIG. 2. Immunocytochemical localization of RUT in semithin cryosections of rat kidney inner and outer medulla. (*A* and *B*) The majority of collecting duct cells are heavily labeled (arrows) whereas some cells, presumably intercalated cells (arrowheads), are unlabeled. Within collecting duct principal cells, RUT labeling is localized to the apical plasma membrane domains and to intracellular vesicles (arrows). (*C*) Collecting duct cells from the mid-inner medulla exhibit extensive RUT-labeling of apical plasma membrane domains and of intracellular vesicles (arrows). (*D*) Localization of RUT in the outer medulla near the junction with the inner medulla. Descending thin limbs in the inner stripe are heavily labeled with labeling of both apical and basal domains (arrows). The papillary surface epithelium (arrowheads) and thick ascending limbs (T) are unlabeled. (*E*) RUT labeling in the inner stripe of the outer medulla. Labeled descending thin limbs are seen in the periphery of a vascular bundle. Arrows indicate an abrupt transition of labeled descending thin limb into an unlabeled thick ascending limb. (*F*) Abrupt transition from distal parts of a labeled decending thin limb into a thick ascending limb (arrows). (*G*) Abrupt transition between unlabeled and labeled portions of descending thin limb (arrows). (*H*) Preadsorption control from the inner medulla. (*I*) Preadsorption control from the outer medulla. [×600 (*A*) and ×1000 (*B-I*)].

thermore, the absence of labeling of some short-loop descending thin limbs as well as the presence of abrupt transitions from unlabeled to labeled thin limb segments (Fig. 2*G*) indicates that the RUT-antibody does not label the entire length of the short-loop descending limb. Rather, labeling appears to be confined to the terminal portion of the short-loop descending thin limb. In contrast to the medulla, there was no immunoperoxidase labeling of any structure in the cortex (not shown).

To determine the subcellular localization of RUT in IMCD cells, immunoelectron microscopy of ultrathin cryosections was carried out. RUT labeling was observed in the apical plasma membrane (Fig. 3*A*). In addition, abundant labeling of intracellular vesicles was observed (Fig. 3 *A* and *B*), mainly in the subapical region. Immunolabeling controls were negative (Fig. 3*A*, *inset*). In contrast to the apical labeling, no labeling of the basolateral plasma membrane of IMCD principal cells was observed (Fig. 3*C*).

We have recently shown that plasma membranes and intracellular vesicles from collecting ducts can be partially separated by sequential centrifugation at 17,000 × *g*, which selectively pellets the plasma membranes, and then at 200,000 × *g*, which selectively pellets the membranes associated with small intracellular vesicles (11, 18). Fig. 4 shows the application of this approach in rat inner medullary homogenates to determine the distribution of RUT among subcellular fractions. As shown, the distribution of RUT is similar to that of aquaporin-2, which is found both in intracellular vesicles and apical plasma membrane (16, 17). That is, a substantial amount of RUT was found in the vesicle-enriched fraction (200,000 × *g*). The distribution of RUT among the fractions contrasts with that of aquaporin-3, a plasma membrane marker (18), which is seen only in the low speed plasma membrane-enriched fractions (Fig. 4). Thus, the findings from subcellular fractionation studies are consistent with the results from immunoelectron microscopy demonstrating the presence of RUT in intracellular vesicles as well as in plasma membranes.

DISCUSSION

In this report, we characterize the regional, cellular, and subcellular distribution of the RUT urea transporter protein in rat kidney. To achieve this goal, we have raised a polyclonal antibody to RUT by immunizing rabbits with a synthetic peptide corresponding to the carboxyl-terminal 19 amino acids of the predicted polypeptide sequence. This sequence is distinct from that of the recently-cloned erythrocyte urea transporter (19), and based on BLAST analysis, has no significant overlap with any other known eukaryotic protein. Supporting the view that the antibody is specific for RUT in the kidney, immunoblots revealed a single band of apparent molecular mass 97 kDa that was not present when the antibody was preadsorbed with the immunizing peptide or when preimmune IgG was substituted. As discussed below, the apparent molecular mass of the labeled protein (97 kDa) is consistent with the size predicted from the open reading frame of a cDNA cloned from the larger of two transcripts expressed in the rat inner medulla. The predominance of the 97-kDa band in the inner medulla (inner medullary tip>base) (Fig. 1*B*) matches well with the results of isolated perfused tubule studies showing rapid, vasopressin-regulated urea transport only in the terminal part of the IMCD.

The open reading frames of the original cDNA clones for rabbit (14) and rat (15) RUT predicted a protein with a molecular mass of approximately 43 kDa. However, Northern blotting using these cDNAs revealed two distinct transcripts; one 2.9 kb in length corresponding to the approximate size of the cloned cDNA and another 4.0 kb in length (14, 15). The 4.0-kb transcript has recently been cloned (C. Shayakul, A. Steel, and M.A.H., personal communication). This longer cDNA contains the entire coding region of the 2.9-kb transcript. Furthermore, the 4.0-kb transcript is extended at the 5′ end, giving an open reading frame that is approximately twice as long as that of the 2.9-kb transcript, indicating that it codes for a much larger protein. Reverse transcription-PCR experiments using microdissected tubule segments demonstrated that the longer transcript is expressed only in the IMCD (20). Thus, the 4-kb transcript expressed in the IMCD fully accounts for the 97 kDa-band found in the rat inner medulla by immunoblotting with our anti-RUT antibody.

The regional localization of RUT demonstrated by immunoblotting (Fig. 1) corresponds well with immunohistochemical localization of RUT along the collecting duct system (Fig. 2) showing RUT restricted to the IMCD. In accord with observations in isolated perfused tubule studies that vasopressin-regulated urea transport occurs primarily in the deeper parts of the IMCD, the labeling of the IMCD principal cells was considerably heavier in the deep parts of the IMCD than in the initial parts close to the outer–inner medullary border. As described previously (1, 21), a high urea permeability restricted to the most terminal part of the collecting duct system is instrumental to the generation of a hypertonic renal medullary interstitium because it delivers large quantities of urea to the region of the medulla with the lowest effective blood flow, thus permitting interstitial urea accumulation.

Both immunocytochemistry (Fig. 2) and immunoelectron microscopy (Fig. 3) demonstrated a predominant apical localization of RUT in IMCD cells. The apical plasma membrane is rate-limiting for overall transepithelial urea transport and manifests a large increase in urea permeability in response to vasopressin (9). Our immunolocalization results therefore support the view that RUT is the "vasopressin-regulated urea transporter" of the apical plasma membrane as suggested previously from (*i*) the similarity between the urea transport properties of intact collecting ducts and *Xenopus* oocytes after injection of RUT cRNA (14) and (*ii*) the high level of expression of RUT mRNA in the IMCD (14). Because physiological studies have also demonstrated phloretin-sensitive urea transport across the basolateral plasma membrane of IMCD cells (6, 9), the absence of demonstrable basolateral labeling with our anti-RUT antibody suggests that the basolateral transport may be mediated by another transporter, perhaps an as-yet-unidentified RUT homologue.

Immunoelectron microscopic studies, employing the immuno-gold technique in ultrathin cryosections, demonstrated labeling both in the apical plasma membrane and in small intracellular vesicles located chiefly in the apical aspect of the IMCD cells. This distribution is very similar to that of the vasopressin-regulated water channel, aquaporin-2 (10, 16, 17). These findings were corroborated by subcellular fractionation experiments (Fig. 4) showing a substantial amount of RUT in the high-speed, intracellular vesicle-enriched pellet (200,000 × *g*) as well as in the low-speed, plasma membrane-enriched pellets, virtually matching the distribution of aquaporin-2. We have demonstrated, using anti-aquaporin-2 antibodies in isolated perfused IMCD, that vasopressin increases the water permeability of the apical plasma membrane by stimulating the exocytosis of aquaporin-2 containing vesicles, thus inserting the vesicles into the apical plasma membrane (10). The finding of abundant RUT in intracellular vesicles raises the possibility that apical urea permeability is modified by means of regulated exocytosis ("shuttling") of RUT-containing vesicles, as seen for aquaporin-2.

In addition to the collecting ducts, the anti-RUT antibody also labeled one additional structure in the kidney, the descending limb of the short loops of Henle [type 1 descending limb or DTL-1 (22)]. The labeling did not include the entire length of the short-loop descending limb, however, but instead was restricted to the terminal half. This corresponds to the only portion of the thin descending limb in which the

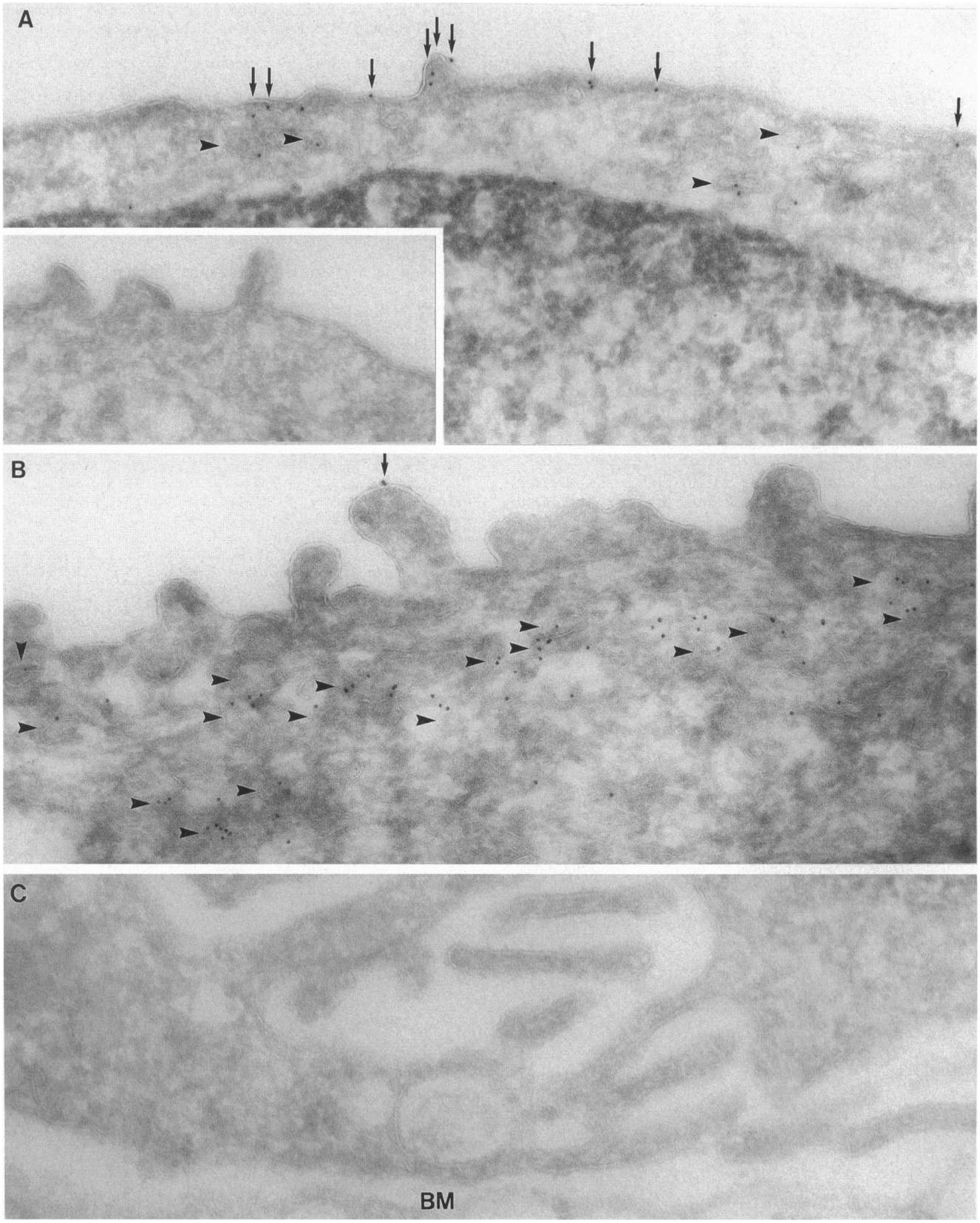

FIG. 3. Immunoelectron microscopical localization of RUT in ultrathin cryosections of IMCD principal cells. (*A* and *B*) Abundant labeling is seen in apical plasma membrane (arrows) and intracellular vesicles (arrowheads). (*C*) Basolateral plasma membranes were unlabeled. Immunolabeling controls using nonimmune IgG is negative (*inset*). BM, basement membrane. (×60,000.)

water channel aquaporin-1 was not demonstrable (23). Thus, the DTL-1 segment is heterogenous. We propose to refer to the early and late parts as DTL-1a and DTL-1b, respectively.

As shown in Fig. 1, immunoblots using membrane fractions from the outer medulla did not reveal any bands. These confirm that RUT is not highly abundant in the outer

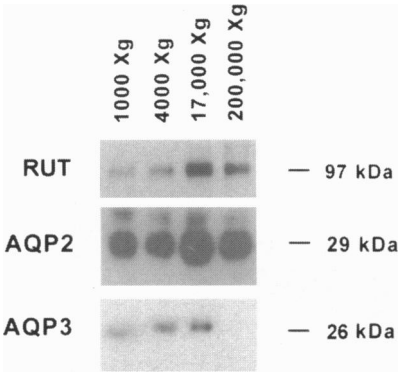

FIG. 4. Subcellular fractionation of inner medullary homogenates. Individual lanes were loaded with membrane fractions prepared by sequential centrifugation at progressively higher speeds. Immunoblots were probed with anti-RUT, or antibodies to the water channels aquaporin-2 or -3. Distribution of RUT between plasma membrane-enriched fraction (17,000 × *g*) and intracellular vesicle-enriched fraction (200,000 × *g*) matched that of aquaporin-2.

medulla, an inevitable consequence of the low abundance of DTL-1b cells.

The DTL-1 segment is difficult to perfuse *in vitro* and consequently relatively little functional data are available to which we can relate the present findings. However, Imai *et al.* (24) did succeed in measuring the urea permeability in a limited number of short-loop descending limbs (DTL-1) from hamster. They demonstrated a urea permeability coefficient in DTL-1 that was approximately 6-fold greater than that of the long-loop descending limb (DTL-2). Rapid urea entry into the short-loop descending limb has been proposed to be important for the maintenance of a high urea concentration in the medulla by providing a pathway for recycling of urea from the medullary blood vessels (the vasa recta) back to the loop of Henle (25, 26). Such a recycling pathway is proposed to retain urea in the medulla that would otherwise be returned to the general circulation via the vasa recta.

We thank Inger Kristoffersen and Trine Møller for expert technical assistance. This work was supported by the intramural budget of the National Heart, Lung, and Blood Institute (National Institues of Health) (J.T., C.S., C.E., and M.K.), as well as the Danish Research Academy, the Novo Nordic Foundation, the Danish Medical Council, and the University of Aarhus Research Foundation (S.N.).

1. Berliner, R. W., Levinsky, N. G., Davidson, D. G. & Eden, M. (1958) *Am. J. Med.* **27,** 730–744.
2. Knepper, M. A. & Rector, F. C., Jr. (1995) in *The Kidney*, eds. Brenner, B. M. & Rector, F. C., Jr. (Saunders, Philadelphia), pp. 532–570.
3. Morgan, T., Sakai, F. & Berliner, R. W. (1968) *Am. J. Physiol.* **214,** 574–581.
4. Sands, J. M., Nonoguchi, H. & Knepper, M. A. (1987) *Am. J. Physiol.* **253,** F823–F832.
5. Star, R. A., Nonoguchi, H., Balaban, R. & Knepper, M. A. (1988) *J. Clin. Invest.* **81,** 1879–1888.
6. Chou, C.-L. & Knepper, M. A. (1989) *Am. J. Physiol.* **257,** F359–F365.
7. Chou, C.-L., Sands, J. M., Nonoguchi, H. & Knepper, M. A. (1990) *Am. J. Physiol.* **258,** F486–F494.
8. Knepper, M. A. & Star, R. A. (1990) *Am. J. Physiol.* **259,** F393–F401.
9. Star, R. A. (1990) *J. Clin. Invest.* **86,** 1172–1178.
10. Nielsen, S., Chou, C.-L., Marples, D., Christensen, E. I., Kishore, B. K. & Knepper, M. A. (1995) *Proc. Natl. Acad. Sci. USA* **92,** 1013–1017.
11. Marples, D., Knepper, M. A., Christensen, E. I. & Nielsen, S. (1995) *Am. J. Physiol.* **269,** C655–C664.
12. Sabolic, I., Katsura, T., Verbabatz, J. M. & Brown, D. (1995) *J. Membr. Biol.* **143,** 165–177.
13. Yamamoto, N., Sasaki, S., Fushimi, K., Ishibashi, K., Yaiota, E., Kawasaki, K., Marumo, F. & Kihara, I. (1995) *Am. J. Physiol.* **268,** C1546–C1551.
14. You, G., Smith, C. P., Kanai, Y., Lee, W.-S., Stelzner, M. & Hediger, M. A. (1993) *Nature (London)* **365,** 844–847.
15. Smith, C. P., Lee, W.-S., Martial, S., Knepper, M. A., You, G., Sands, J. M. & Hediger, M. A. (1995) *J. Clin. Invest.* **96,** 1556–1563.
16. Nielsen, S., DiGiovanni, S. R., Christensen, E. I., Knepper, M. A. & Harris, H. W. (1993) *Proc. Natl. Acad. Sci. USA* **90,** 11663–11667.
17. DiGiovanni, S. R., Nielsen, S., Christensen, E. I. & Knepper, M. A. (1994) *Proc. Natl. Acad. Sci. USA* **91,** 8984–8988.
18. Ecelbarger, C. A., Terris, J., Frindt, G., Echevarria, M., Marples, D., Nielsen, S. & Knepper, M. A. (1995) *Am. J. Physiol.* **269,** F663–F672.
19. Olives, B., Neau, P., Bailly, P., Hediger, M. A., Rousselet, G., Cartron, J. P. & Ripoche, P. (1994) *J. Biol. Chem.* **269,** 31649–31652.
20. Shayakul, C., Knepper, M. A., Smith, C. P., DiGiovanni, S. R. & Hediger, M. A. (1996) *FASEB J.* **10,** A273 (abstr.).
21. Star, R. A. & Knepper, M. A. (1990) *Am. J. Physiol.* **259,** F393–F401.
22. Kriz, W. & Bankir, L. (1988) *Am. J. Physiol.* **254,** F1–F8.
23. Nielsen, S., Pallone, T., Smith, B. L., Christensen, E. I., Agre, P. & Maunsbach, A. B. (1995) *Am. J. Physiol.* **268,** F1023–F1037.
24. Imai, M., Hayashi, M. & Araki, M. (1984) *Pflügers Arch.* **402,** 385–392.
25. Knepper, M. A. & Roch-Ramel, F. (1987) *Kidney Int.* **31,** 629–633.
26. Lemley, K. V. & Kriz, W. (1987) *Kidney Int.* **31,** 538–548